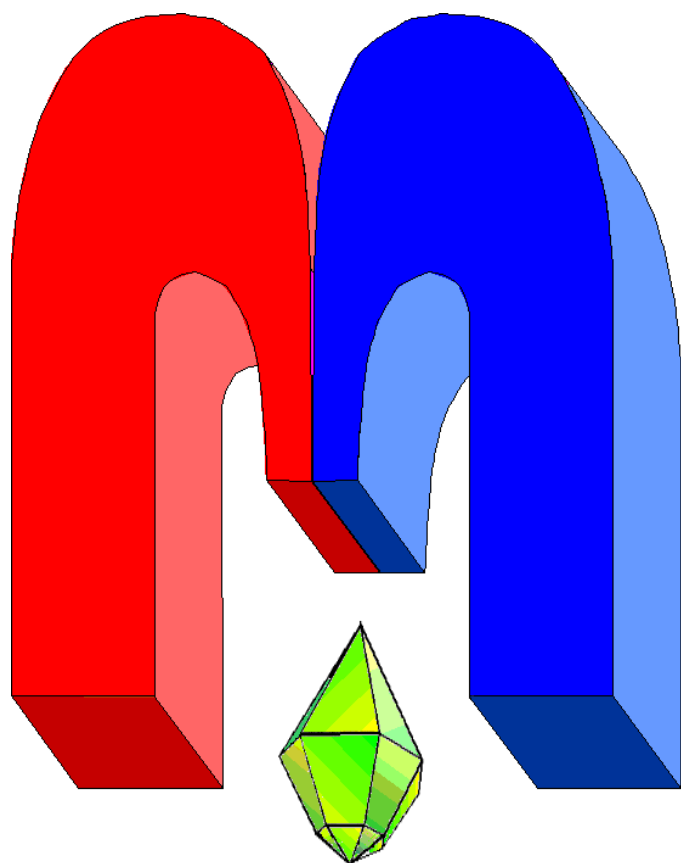


ISSN 2072-5981

doi: 10.26907/mrsej



***magnetic
Resonance
in Solids***

Electronic Journal

Volume 25

Issue 3

Article No 23300

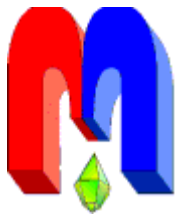
1-8 pages

2023

doi: [10.26907/mrsej-23302](https://doi.org/10.26907/mrsej-23302)

<http://mrsej.kpfu.ru>

<http://mrsej.ksu.ru>



Established and published by Kazan University*
Endorsed by International Society of Magnetic Resonance (ISMAR)
Registered by Russian Federation Committee on Press (#015140),
August 2, 1996
First Issue appeared on July 25, 1997

© Kazan Federal University (KFU)†

"Magnetic Resonance in Solids. Electronic Journal" (MRSej) is a peer-reviewed, all electronic journal, publishing articles which meet the highest standards of scientific quality in the field of basic research of a magnetic resonance in solids and related phenomena.

Indexed and abstracted by
Web of Science (ESCI, Clarivate Analytics, from 2015), Scopus (Elsevier, from 2012), RusIndexSC (eLibrary, from 2006), Google Scholar, DOAJ, ROAD, CyberLeninka (from 2006), SCImago Journal & Country Rank, etc.

Editor-in-Chief

Boris **Kochelaev** (KFU, Kazan)

Honorary Editors

Jean **Jeener** (Universite Libre de Bruxelles, Brussels)

Raymond **Orbach** (University of California, Riverside)

Executive Editor

Yurii **Proshin** (KFU, Kazan)
mrsej@kpfu.ru



This work is licensed under a [Creative Commons Attribution-ShareAlike 4.0 International License](https://creativecommons.org/licenses/by-sa/4.0/).



This is an open access journal which means that all content is freely available without charge to the user or his/her institution. This is in accordance with the [BOAI definition of open access](https://www.boai.ru/).

Technical Editor

Maxim **Avdeev** (KFU, Kazan)

Editors

Vadim **Atsarkin** (Institute of Radio Engineering and Electronics, Moscow)

Yurij **Bunkov** (CNRS, Grenoble)

Mikhail **Eremin** (KFU, Kazan)

David **Fushman** (University of Maryland, College Park)

Hugo **Keller** (University of Zürich, Zürich)

Yoshio **Kitaoka** (Osaka University, Osaka)

Boris **Malkin** (KFU, Kazan)

Alexander **Shengelaya** (Tbilisi State University, Tbilisi)

Jörg **Sichelschmidt** (Max Planck Institute for Chemical Physics of Solids, Dresden)

Haruhiko **Suzuki** (Kanazawa University, Kanazawa)

Murat **Tagirov** (KFU, Kazan)

Dmitrii **Tayurskii** (KFU, Kazan)

Valentine **Zhikharev** (KNRTU, Kazan)

* Address: "Magnetic Resonance in Solids. Electronic Journal", Kazan Federal University; Kremlevskaya str., 18; Kazan 420008, Russia

† In Kazan University the Electron Paramagnetic Resonance (EPR) was discovered by Zavoisky E.K. in 1944.

EPR of catalytic complexes of Mn (II) with sodium pectate

M.K. Kadirov^{1,2}, A.F. Sabirova¹, D.M. Kadirov², R.N. Mansurov^{1,2,*}, S.T. Minzanova^{1,2},
K.V. Kholin^{1,2}, E.I. Galeeva²

¹A.E. Arbuzov Institute of Organic and Physical Chemistry, FRC Kazan Scientific Center,
Russian Academy of Sciences, Kazan 420088, Russia

²Kazan National Research Technological University, Kazan 420015, Russia

*E-mail: ravil545@bk.ru

(Received October 30, 2023; revised December 12, 2023;
accepted December 13, 2023; published December 24, 2023)

Coordination biopolymers, namely, nickel complexes of sodium pectate, have been actively studied in recent years as promising representatives of non-platinum catalysts for proton exchange membrane fuel cells. The structure of coordination polymers consisting of natural precursors is complex and not entirely regular. It presents significant difficulties in determining the internal structure of coordination polymers. Identifiable electron paramagnetic resonance (EPR) signals of various Mn²⁺ units in sodium pectate manganese complexes have provided important structural information in systems similar in composition to nickel coordination biopolymers. In addition, the manganese complexes with the natural pectin polymers themselves are of interest as non-platinum PEMFC catalysts.

PACS: 75.30.Et, 76.50.+g, 76.30.-v, 76.30.FC, 76.30.Rn

Keywords: proton exchange membrane fuel cell, non-platinum catalysts, coordination biopolymers, electron paramagnetic resonance, octahedral environment, “egg-box” structures

1. Introduction

Proton exchange membrane fuel cells (PEMFCs) are platinum catalyst based electrochemical devices and future high energy density vehicle energy alternatives [1, 2]. However, the scarcity, high cost and infinite availability of Pt is a bottleneck in their application [3, 4]. This is due to the slow rate of oxygen reduction reaction (ORR) in the fuel cell due to the low solubility of oxygen gas in water [5]. The ORR rate is five orders of magnitude lower than that of the hydrogen oxidation reaction (HOR) [6]. The main way to increase the reaction rate on the cathode side is a higher the catalyst loading [7–9]. However, this leads to low productivity and low efficiency of Pt use [10].

In addition, commercial carbon-based Pt (Pt/C) has a complex wet chemical process for Pt synthesis [11, 12]. Considering the ever-increasing volumes of Pt production, this is an additional and serious burden on the Earth’s ecosystem. It is not for nothing that the US Department of Energy has proposed an ultra-low Pt content target (total electrode surface density: 0.100 mgPt cm⁻²) by 2025 [13]. It is critical to increase Pt utilization by providing a larger catalyst surface area with a small amount of this precious metal. However, this is, firstly, a rather difficult task, and secondly, a decrease in Pt in the catalytic layer usually leads to a deterioration in the stability of the catalyst. All of the above has led to recent scientific research also focusing on the development of catalysts that do not contain platinum group metals.

Several years ago, research on nickel complexes of sodium pectate began and, on their basis, the first ORR catalysts for PEMFC were obtained from these coordination pectin biopolymers obtained from agricultural and food waste [14–16]. Continuous reproduction of the precursors on a large scale by nature itself, low cost, biodegradability and low environmental impact make coordination biopolymers an interesting class of catalysts for hydrogen energetics. Complexes

of Ni^{2+} with sodium pectate are “EPR-silent” under normal conditions, and such a powerful method as EPR cannot be used when studying the parent compounds. Our preliminary studies have shown that the divalent manganese ion Mn^{2+} forms complexes with sodium pectate and produces clear EPR spectra at room temperature. This article is devoted to the use of the EPR method for the study of Mn^{2+} complexes with sodium pectate, which also showed noticeable catalytic properties in ORR.

The properties of coordination biopolymers are mainly determined by the degree of local order/disorder. Therefore, studies that provide local structure information are important to understand the correlation between catalytic properties and structure. Electron paramagnetic resonance is one of the most powerful methods for studying local order and magnetic interactions [17]. As a rule, the EPR spectra of Mn^{2+} ions ($3d^5$; ${}^6\text{S}_{5/2}$; $I = 5/2$) in glassy media consist of spectral lines centered at $g_{\text{eff}} \approx 5.1, 3.0$ and 2 , the ratio of their intensities varies depending on the composition [18, 19]. It should be noted that due to the large value of the hyperfine interaction of manganese ions, the center of the EPR spectrum shifts to weaker fields. Therefore the calculation of g -factor based on the position of the center of the EPR spectrum gives overestimated values and in the future we will denote them as g_{eff} . Calculation of the real g -factor for the Zeeman interaction requires approximation of EPR spectra and will be done in the following publications. The EPR line at $g_{\text{eff}} \approx 5.1$ corresponds to isolated Mn^{2+} ions located in slightly tetragonally or orthorhombically distorted cubic symmetric sites [20]. The signal at $g_{\text{eff}} \approx 3.0$ is characteristic of isolated Mn^{2+} ions located in an octahedral neighborhood exposed to strong crystal fields [18–21]. Resonant absorption $g_{\text{eff}} \approx 2.0$ can be attributed to isolated ions, as well as ions participating in dipole [22] and/or superexchange magnetic interactions [20].

2. Materials and methods

2.1. Synthesis of the sodium pectate complexes with manganese

The synthesis of the complexes was carried out according to a known method [23–26]. The synthesis scheme is shown in Figure 1a. At the first stage, by treating citrus pectin with alkali, sodium pectate (NaPG) was obtained with a degree of salt formation of 100%.

The obtained sodium pectate (Figure 1b) was the starting ligand for the synthesis of metal complexes, and then the target compounds were synthesized using the reaction of ligand exchange of Na^+ ions for Mn^{2+} cations. The experiments were planned in such a way as to create a rarefied three-dimensional structure of the complexes with a relatively low degree of substitution of sodium ions for d-metal while maintaining most of the sodium ions in salt form in the composition of the polymer complex to ensure its water-soluble properties (within $5 \div 25\%$ divalent metal manganese relative to the initial content of monovalent sodium).

2.2. Electron paramagnetic resonance

EPR measurements were carried out on the Bruker Elexsys E-500 spectrometer utilizing a 100 kHz field modulation and X-band microwaves. The operating frequency of the spectrometer is 9.672 GHz.

2.3. X-ray diffraction (XRD) analysis

Powder X-ray diffraction patterns were obtained on a Rigaku SmatLab X-ray diffractometer. Cu K-alpha₁ radiation ($\lambda = 1.54063 \text{ \AA}$) was used, X-ray tube operating mode was 45 kV, 200 mA. Experiments were performed at room temperature. The sample was filled into the recess of a standard cuvette. Diffraction patterns were recorded in the range of scattering angles 2θ is $5 \div 100^\circ$, at a speed of 1 deg/min.

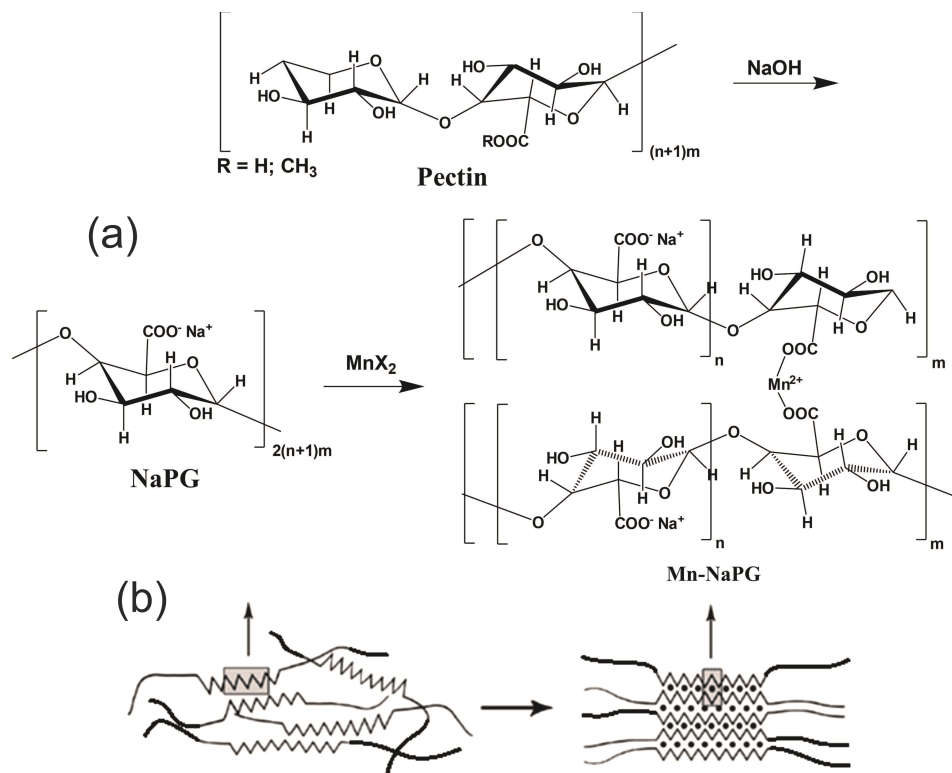


Figure 1. Schemes for the synthesis of pectin polysaccharide complexes ($n = 3 \div 10$, $m = 10 \div 35$, n and m - the length of pectin polysaccharide complexes) with manganese (II) (a) and the formation of polymer-complex structures according to the “egg-box” model (b).

3. Results and discussion

Figure 2 shows the EPR spectra of Mn^{2+} ions in $\text{Mn}(n\%)\text{-NaPG}$ coordination bio-polymer powders. The spectra show resonance lines due to paramagnetic Mn^{2+} in the range Na substitution of $5 \div 25\%$, which are centered at the $g_{\text{eff}} \approx 2.0$, 3.0 and 5.1 . These values are very close to the g values for 1% Mn^{2+} in glasses of the systems $\text{B}_2\text{O}_3 - \text{BaO}$ [27]. Signals at $g_{\text{eff}} \approx 2.0$ are clearly distinguishable and noticeable changes in the shape and intensity of the lines are visible from them. The intensity of the resonance signal at $g_{\text{eff}} = 2.0$ from the $\text{Mn}(5\%)\text{-NaPG}$ coordination biopolymer is the lowest among the corresponding signals from other samples with a higher content of Mn^{2+} ions, and a noticeable hyperfine structure is superimposed on this line, which also manifests itself in the $\text{Mn}(10\%)\text{-NaPG}$ sample. It is known that the resonance line $g_{\text{eff}} \approx 2.0$ arises from the central transition $M_s = |-1/2\rangle \rightarrow |+1/2\rangle$, where M_s is the effective spin component. The multiplet of six lines (Figure 3) is the result of hyperfine interaction of the electron spin with the nucleus of the ^{55}Mn isotope ($I = 5/2$). The close to octahedral symmetry environment around the isolated Mn^{2+} ion leads to this isotropic signal with $g_{\text{eff}} = 2.0$. The hyperfine structure (Figure 3) with the hyperfine interaction constant $A \approx 118 \text{ G}$ and the above g_{eff} indicate the predominantly ionic nature of the bond between Mn^{2+} and O^{2-} ions, generating a ligand field with octahedral symmetry. The possibility of superimposing weak axial distortions on this field was also shown [28, 29].

As can be seen from the $\text{Mn}(5\%)\text{-NaPG}$ spectrum in Figure 2, the hyperfine structure is superimposed on the large absorption line. This resulting signal can be considered as the envelope of all resonance absorption contributions at magnetic field correspondent to $g_{\text{eff}} \approx 2.0$ caused by the random distribution of Mn^{2+} in the powder matrix of the coordination biopolymer. As the Mn^{2+} content increases, the hyperfine structure blurs [Figure 2, from $\text{Mn}(10\%)\text{-NaPG}$ to

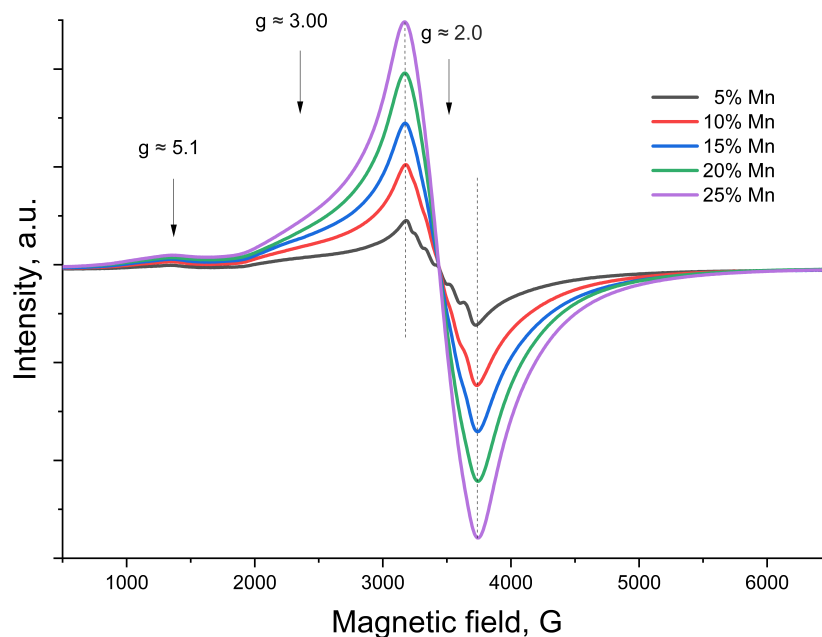


Figure 2. EPR spectra of Mn^{2+} ions in $\text{Mn}(n\%)\text{-NaPG}$ coordination biopolymers.

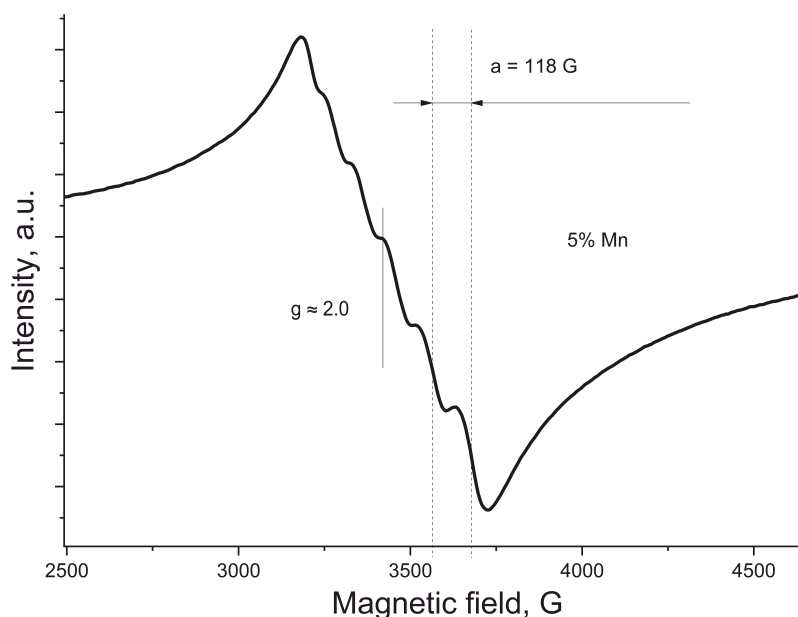


Figure 3. EPR spectrum of Mn^{2+} ions in $\text{Mn}(5\%)\text{-NaPG}$ powder.

$\text{Mn}(25\%)\text{-NaPG}$]. This is due, firstly, to the distribution of crystal field parameters, and secondly, to an increase in viscosity due to the increasing number of cross-links of the coordination biopolymer with a divalent transition ion, as well as dipole-dipole interaction accompanied by magnetic superexchange.

In the case of the glass system $x\text{MnO}(100x)[y\text{P}_2\text{O}_5 \text{CaO}]$ [30] with $y = 1$ and 2, the line width increases with the MnO content up to $x = 5$ and 10 mol%, respectively, due to an increase in the dipole interaction between Mn^{2+} ions. For higher concentrations from $x \geq 10$ up to 50 mol%, a strong decrease in the linewidth can be observed, which can be attributed to the superexchange type of interaction between manganese ions quite close to each other. Such degrees of doping of

samples cause increasing clustering of manganese ions. In the case of our systems, the picture is completely different. The width of the intense line at $g_{\text{eff}} \approx 2.0$ does not change over the entire studied range of Mn^{2+} ion concentrations, which is clearly visible in Figure 2. This behavior can be explained by the fact that clustering in our case comes down to the collapse of sites with the Mn^{2+} cation into structures where the distance between the ions and their immediate environment no longer changes with increasing concentration of transition metal, but only the number and/or size of these clusters increase. Such clusters with tightly packed Ca^{2+} nodes surrounded by four galacturonic acids were previously studied [31] by recording changes in the circular dichroism spectra and were called “egg-boxes”. It can be assumed on the EPR data that the present study confirms the formation of the “egg-boxes” in Mn-NaPG systems. It was recently [32] found that in the case of calcium (Ca) and Mn ions, their concentration does not affect their distribution in the alginate structure and the cross-linking density.

Highly distorted versions of the octahedral neighborhood, subjected to strong crystal field influence [33,34], cause absorption at $g_{\text{eff}} \approx 5.1$ and 3.0 (Figure 2). Figure 4 shows the low-field Mn^{2+} EPR spectra, normalized to the most intense component at $g_{\text{eff}} \approx 2.0$. Fragments of these spectra, enlarged (in the inset) around $g_{\text{eff}} \approx 5.1$, show that they are more pronounced at low concentrations of the Mn^{2+} .

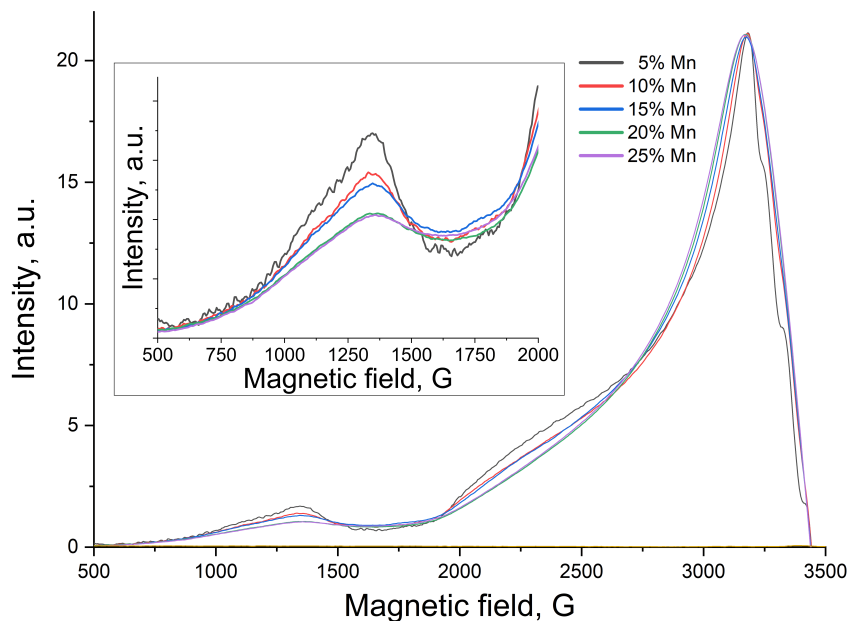


Figure 4. Low-field EPR spectra of Mn^{2+} ions in Mn(n%)-NaPG coordination biopolymers, normalized by the most intense component at $g_{\text{eff}} \approx 2.0$, and an enlarged fragment of this spectrum (in the inset) around $g_{\text{eff}} \approx 5.1$.

Depending on the Mn^{2+} content, the structure of the coordination biopolymers shows the evolution of structural units with these ions in well-defined neighborhoods to structural units containing clustered magnetic ions. The intensities of the lines at $g_{\text{eff}} \approx 5.1$ and 3.0 are quite low and indicate a relatively low concentration of isolated Mn^{2+} ions that are part of structural units with a strongly distorted octahedral neighborhood.

Figure 5 presents the results of the XRD study. The XRD pattern of Mn(5%)-NaPG in the range of $10 \div 50^\circ$ exhibits interference peaks (albeit somewhat broadened) corresponding to the crystalline phase. An increase in the concentration of manganese leads to a slight disordering

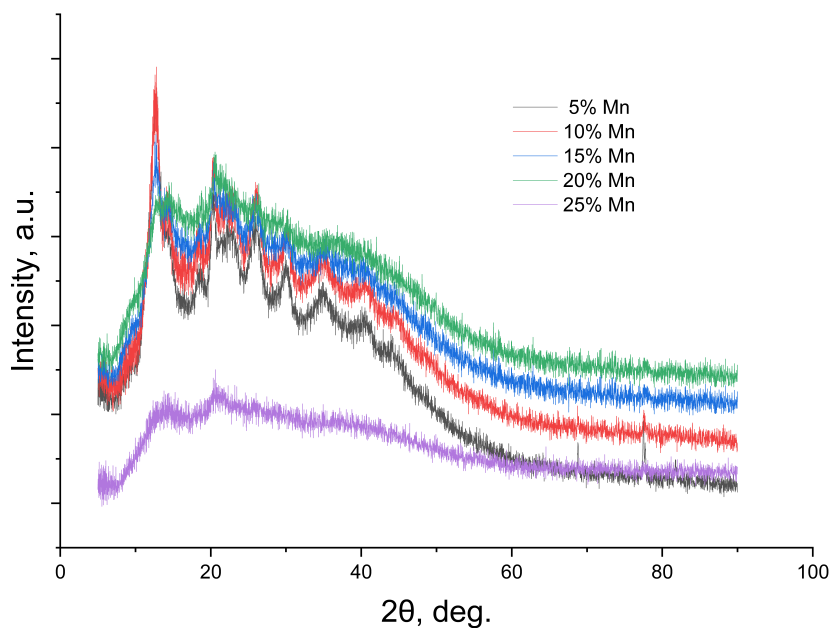


Figure 5. Experimental diffraction patterns for Mn(n%)-NaPG

Table 1. Degree of crystallinity of the Mn(n%)-NaPG.

Sample	Degree of crystallinity, %
Mn(5%)-NaPG	23.9
Mn(10%)-NaPG	20.16
Mn(15%)-NaPG	15.1
Mn(20%)-NaPG	8.5
Mn(25%)-NaPG	5.6

of crystalline fragments, which is expressed in a significant broadening and even disappearance of some peaks. The amorphous phase grows. Table 1 clearly shows a gradual decrease in the degree of crystallinity from 23.9% for Mn(5%)-NaPG to 5.6% for Mn(25%)-NaPG. These studies confirm the above results of using the EPR method, namely, the evolution of structural units with Mn^{2+} ions in more crystalline surroundings to more amorphous structural units containing magnetic clusters.

4. Conclusion

Complexes of Mn^{2+} with sodium pectate were studied by EPR in the range of transition metal ion concentrations of 5-25%. Resonance lines centered on $g_{\text{eff}} \approx 2.0$, 3.0 and 5.1 were recorded. EPR spectra revealed the distribution of Mn^{2+} ions in a number of structural units of coordination biopolymers depending on the Mn^{2+} content. The close to octahedral symmetry of the environment around an isolated Mn^{2+} ion leads to an isotropic signal with $g_{\text{eff}} = 2.0$ and $A \approx 118$ G. It indicates the predominantly ionic nature of the bond between Mn^{2+} and O^{2-} , generating a ligand field with octahedral symmetry. Distorted versions of the octahedral neighborhood, subject to the strong influence of the crystal field, cause absorptions at $g_{\text{eff}} \approx 5.1$ and 3.0, which are more pronounced at low Mn^{2+} concentrations. The intensities of the lines at $g_{\text{eff}} \approx 5.1$ and 3.0 are quite low and indicate a relatively low concentration of isolated Mn^{2+}

ions, which are part of structural units with a strongly distorted octahedral neighborhood.

XRD studies confirm the results of the EPR method, namely, the evolution of structural units with Mn^{2+} ions in more crystalline surroundings to more amorphous structural units containing magnetic clusters with increasing of manganese concentration.

The constancy of the line width of the intense at $g_{\text{eff}} \approx 2.0$ throughout the studied range of Mn^{2+} concentrations is explained by the fact that clustering is reduced to such a dense structuring of sites with the Mn^{2+} ion, where the distance between the ions and their immediate environment does not change with increasing concentration of the transition metal, and only the number and/or size of these clusters increase. The present study confirms the formation of such “egg-box” structures in Mn-NaPG systems.

Acknowledgments

The reported study was funded by RSF, project number 22-29-00895.

References

1. Steele B. C. H., Heinzl A. *Nature* **414**, 345 (2001)
2. Perry M. L., Fuller T. F. *J. Electrochem. Soc.* **149**, S59 (2002)
3. Debe M. K. *Nature* **486**, 43 (2012)
4. Stephens I. E. L., Rossmeisl J., Chorkendorff I. *Science* **354**, 1378 (2016)
5. Parthasarathy A., Srinivasan S., Appleby A. J., Martin C. R. *J. Electrochem. Soc.* **139**, 2530 (1992)
6. Jaouen F., Proietti E., Lefèvre M., Chenitz R., Dodelet J. P., Wu G., Zelenay P. *Energy Environ. Sci.* **4**, 114 (2011)
7. Singh H., Zhuang S., Ingis B., Nunna B. B., Lee E. S. *Carbon* **151**, 160 (2019)
8. Wang C., Markovic N. M., Stamenkovic V. R. *ACS Catal.* **5**, 891 (2012)
9. Osmieri L., Park J., Cullen D. A., Zelenay P., Myers D. J., Neyerlin K. C. *Curr. Opin. Electrochem.* **25**, 100627 (2021)
10. Oh H. S., Oh J. G., Hong Y. G., Kim H. *Electrochim. Acta* **52**, 7278 (2007)
11. Alekseenko A. A., Guterma V. E., Tabachkova N. Y., Safronenko O. I. *J. Solid State Electrochem.* **21**, 2899 (2017)
12. Alekseenko A. A., Ashihina E. A., Shpanko S. P., Volochaev V. A., Safronenko O. I., Guterma V. E. *Appl. Catal., B* **226**, 608 (2018)
13. Thompson S. T., Wilson A. R., Zelenay P., Myers D. J., More K. L., Neyerlin K. C., Papageorgopoulos D. *Solid State Ionics* **319**, 68 (2018).
14. Kadirov M. K., Minzanova S., Nizameev I., Mironova L. G., Gilmutdinov I., Khrizanforov M., Kholin K., Khamatgalimov A., Semeonov V., Morozov V., Kadirov D. M., Mukhametzyanov A., Budnikova Yu., Sinyashin O. *Inorg. Chem. Front.* **5**, 780 (2018)
15. Kadirov M. K., Minzanova S. T., Nizameev I. R., Khrizanforov M. N., Mironova L. G., Kholin K. V., Kadirov D. M., Nefed'ev E. S., Morozov M. V., Gubaidullin A. T., Budnikova Yu. H., Sinyashin O. G. *Chem.Sel.* **4**, 4731 (2019)

16. Nizameev I. R., Kadirov D. M., Nizameeva G. R., Sabirova A. F., Kholin K. V., Morozov M. V., Mironova L. G., Zairov R. R., Minzanova S. T., Sinyashin O.G., Kadirov M. K. *Int. J. Mol. Sci.* **23**, 14247 (2022)
17. Griscom D. L. *J. Non-Cryst. Solids* **40**, 211 (1980)
18. Loveridge D., Parke S. *Phys. Chem. Glasses* **12**, 19 (1971)
19. Černý V., Petrová B., Frumar M. *J. Non-Cryst. Solids* **125**, 17 (1990)
20. Ardelean I., Peteanu M., Ilonca G., *Phys. Stat. Solidi A* **58**, K33 (1980)
21. Schreurs J. W. H. *J. Chem. Phys.* **5**, 2151 (1978)
22. Cozar O., Ardelean I., Ilonca G. *Solid State Commun.* **44**, 809 (1982)
23. Minzanova S. T., Mironov V. F., Vyshtakalyuk A. B., Tsepaeva O. V., Mironova L. G., Mindubaev A. Z., Milyukov V. A. *Carbohydr. Polym.* **134**, 523 (2015)
24. Minzanova S. T., Khamatgalimov A. R., Ryzhkina I. S., Murtazina L. I., Mironova L. G., Kadirov M. K., Mironov V. F. *Dokl. Phys. Chem.* **467**, 45 (2016)
25. Kuzmann E., Garg V. K., De Oliveira A. C., Klencsar Z., Szentmihalyi K., Fodor J., Homonnay Z. *Radiat. Phys. Chem* **107**, 195 (2015)
26. Assifaoui A., Lerbret A., Uyen H. T., Neiers F., Chambin O., Loupiac C., Cousin F. *Soft Matter* **11**, 551 (2015)
27. Nicklin R. C., Farach H. A., Poole C. P. *J. Chem. Phys.* **65**, 2998 (1976)
28. Peteanu M., Ardelean I., Filip S., Alexandru D. *Rom. Rep. Phys.* **41**, 593 (1996)
29. Ardelean I., Filip S. *J. Optoelectron. Adv. Mater.* **5**, 157 (2003)
30. Toloman D., Giurgiu L. M., Ardelean I. *Physica B* **21**, 4198 (2009)
31. Grant G. T., Morris E. R., Rees D. A., Smith P. J., Thom D. *FEBS Lett.* **32**, 195 (1973)
32. Forysenkova A. A., Ivanova V. A., Fadeeva I. V., Mamin G. V., Rau J. V. *Mater.* **16**, 2832 (2023)
33. Černý V., Frumarova B., Borsa J., Licholit I. L., Frumar M., *J. Non-Cryst. Solids* **192**, 165 (1995)
34. Ardelean I., Ilonca G., Peteanu M. *Solid State Commun.* **52**, 147 (1984)